STATISTICAL MODELING OF PEAK ACCELERATING GRADIENTS IN LCLS-II AND LCLS-II-HE*

J.T. Maniscalco†, S. Aderhold, J.D. Fuerst, D. Gonnella
SLAC National Accelerator Laboratory, Menlo Park, CA, USA
T.T. Arkan, M. Checchin, J.A. Kaluzny, S. Posen, Fermilab, Batavia, IL, USA
J. Hogan, A.D. Palczewski, C. E. Reece, K.M. Wilson, JLab, Newport News, VA, USA

Abstract

In this report, we study the vertical test gradient performance and the gradient degradation between vertical test and cryomodule test for the 1.3 GHz LCLS-II cavities. We develop a model of peak gradient statistics, and use our understanding of the LCLS-II results and the changes implemented for LCLS-II-HE to estimate the expected gradient statistics for the new machine. Finally, we lay out a plan to ensure that the LCLS-II-HE cryomodule gradient specifications are met while minimizing cavity disqualification by introducing a variable acceptance threshold for the accelerating gradient.

MODELING LCLS-II CAVITY GRADIENT PERFORMANCE

Our study begins with the vertical test results from the 1.3 GHz nine-cell SRF cavities built for the LCLS-II project. These cavities were prepared with the "2/6" nitrogen doping recipe (also called "2N6") described in previous work [1]. Figure 1 shows the distribution of peak accelerating gradients measured for the LCLS-II cavities in vertical test, measured after processing of any field emission or multipacting encountered. It should be noted that some LCLS-II cavity tests were performed while an administrative limit on gradient was in place; these artificially limited cavities have been omitted from this study. The results depicted here therefore represent the ultimate gradient limits of the LCLS-II cavities.

We can understand this distribution using a two-parameter thermal defect model, based on the thermal defect model developed at Saclay [2]. In this model, thermal defects are distributed across the surface of the cavity, and each cavity's ultimate gradient limitation is determined by the largest such defect. The cumulative probability distribution function of the size ϕ, with normalization constant ϕ_0, of the largest defect is given by the following:

$$P(\phi) = \exp\left(-s\left(\frac{\phi}{\phi_0}\right)^{-m}\right) \tag{1}$$

Fit parameter s relates to the total number of defects on the surface, with larger s corresponding to a higher overall number of defects; parameter m relates to the size distribution of
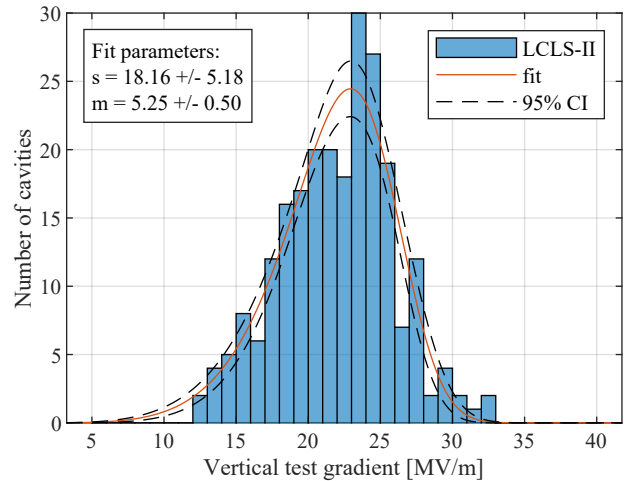

Figure 1: Distribution of peak gradients achieved by LCLS-II cavities in vertical test after administrative limit was removed. Also shown is the model with fitted parameters and 95% confidence interval.

defects, with larger m corresponding to more small defects and fewer large defects. We differentiate Eq. 1 to give the probability density function:

$$p(\phi) = \exp\left(-s\left(\frac{\phi}{\phi_0}\right)^{-m}\right) \frac{s\,m}{\phi_0}\left(\frac{\phi}{\phi_0}\right)^{-m-1} \tag{2}$$

As suggested by the fit to experimental data presented in the Saclay paper, we take the quench field B_q of a cavity with largest defect of size ϕ and a superheating critical field B_{sh} as follows:

$$b(\phi) = \frac{B_q}{B_{sh}} = \left(1 + \left(\frac{\phi}{\phi_0}\right)^2\right)^{-1/2} \tag{3}$$

Then combining the above we can determine the the probability density function of b, which is defined over the interval $(0, 1)$:

$$p(b) = \exp\left(-s\left(b^{-2}-1\right)^{-m/2}\right) \frac{s\,m}{b^3}\left(b^{-2}-1\right)^{-m/2-1} \tag{4}$$

We note that the defect size and normalization parameter have dropped out, leaving us with the defect parameters s and m as well as the superheating field B_{sh} included in the definition of b.

From this probability density we further account for normally distributed measurement error to arrive at the final probability distribution of the measured quench field b_{meas}:

$$p(b_{\text{meas}}) = \int_0^1 p(b) \frac{1}{\sigma' b \sqrt{2\pi}} \exp\left(-\frac{1}{2}\left(\frac{b_{\text{meas}} - b}{\sigma' b}\right)^2\right) db \quad (5)$$

Here, $p(b)$ has been convoluted with a normal distribution with standard deviation σ'. Approximating $B_{\text{sh}} = 200$ mT as a reasonable estimate for lightly-doped niobium [3] and a measurement uncertainty of 5%, consistent with experience and an error analysis performed for the methods used to obtain these results [4, 5], we can fit s and m to the distribution of cavity gradients, resulting in the line plotted in Fig. 1. Notably, our fitted value of $m = 5.25$ is consistent with the $m = 5$ found at Saclay for other 1.3 GHz niobium cavities [2].

With a model of the vertical test performance in hand, we can turn to the limitations to peak gradient in the LCLS-II cavities as measured after cryomodule assembly. Figure 2 shows the distribution of "usable" gradients achieved by the cavities studied above (*i.e.* still excluding cavities tested vertically with the artificial administrative limit) in the cryomodule tests, excluding the cavities that were rejected from string assembly (mostly those that did not reach 18 MV/m in vertical test). The "usable gradient" of a cavity, as defined by LCLS-II, refers to the highest gradient where stable operation is possible without quenching or field-emitting beyond tolerance, minus 0.5 MV/m, subject to an overall administrative limit of 21 MV/m. Each cavity is labeled according to the reason for the limitation as identified by the cryomodule test operator:

- "FE limit": limited due to detection of field emission, radiation, dark current, etc. beyond allowable threshold, or exhibited radiation and had a usable gradient lower than the maximum gradient

- "admin limit": reached administrative limit, not limited by quench, and exhibited no field emission

- "quench usable limit": limited by quench with usable gradient recorded by operator greater than 0.5 MV/m less than maximum gradient (*i.e.* stable operation above the recorded usable gradient was not possible for the hour required)

- "quench limit": limited by quench and not falling into above categories

- "all other limits": not falling into any of the above categories

The usable gradient distribution rises sharply at 17 MV/m, the start of the multipacting band for TESLA cavities [6], in particular driven by an increase in "quench usable limit" cavities. The unstable operation of these cavities indicated by the "quench usable limit" conditions is a signature of
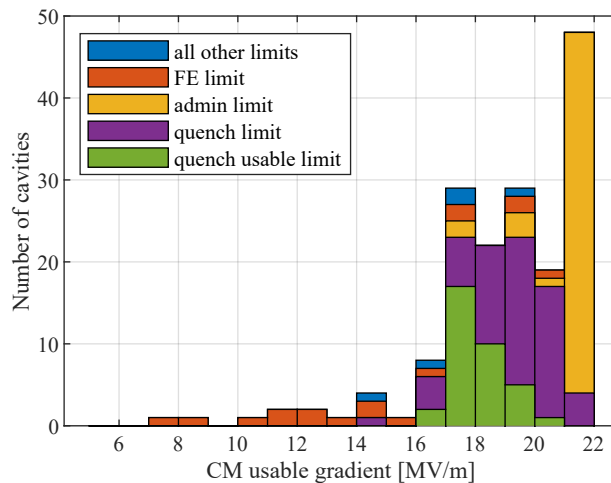

Figure 2: Stacked histogram of the distribution of limits to the usable accelerating gradient of LCLS-II cavities installed in cryomodules.

multipacting, suggesting that unprocessed multipacting was indeed the limiting factor for many of the cavities. Moreover, during LCLS-II cryomodule production, cavities quenching above the target module gradient of 16 MV/m were often not processed for potential multipacting. From this we may suppose that many cavities quenching in the 17-21 MV/m range during cryomodule testing were not pushed to their ultimate limit, and that the usable gradient of these cavities was artificially reduced from the limit observed in vertical test due to a lack of processing multipacting. In total, approximately 50% of all cavities represented here were limited in this range with no steady radiation signal, consistent with multipacting, with their usable gradients distributed approximately uniformly over the multipacting band.

Looking at the other limits, approximately 5% of cavities were limited by field emission, with the field emission limitation field distributed approximately uniformly from 7 MV/m up to the administrative limit.

We can numerically simulate the usable gradients as measured in the cryomodule test by generating a set of virtual cavities with ultimate gradient limits distributed according to Eq. 5, removing cavities which did not reach the vertical test acceptance criterion, statistically assigning limitation by field emission and multipacting over the aforementioned ranges, and finally imposing the administrative limit. The usable gradient of each simulated cavity is the lowest of its defect-limited peak gradient, the administrative limit, and its field emission onset field and multipacting field (if any). The results of this simulation, with 50% of cavities limited by multipacting and 5% limited by field emission, are shown in Fig. 3. Here, the total number of cavities has been increased by a factor of 10 to reveal the underlying statistical distribution. The simulation results agree well with the experimental results from LCLS-II.
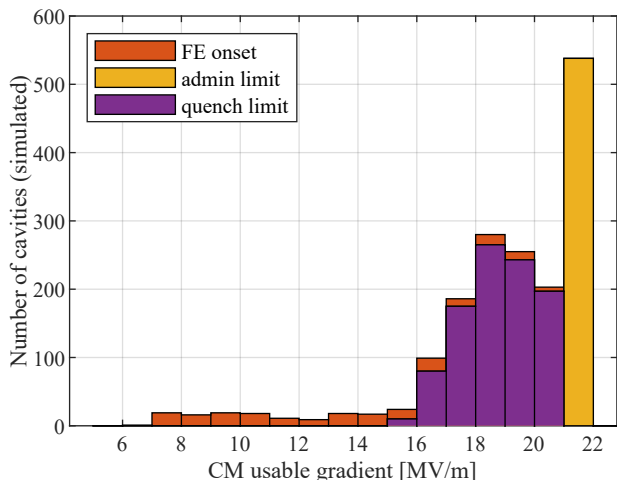
Figure 3: Usable gradient limit distribution for simulation with parameters emulating LCLS-II.
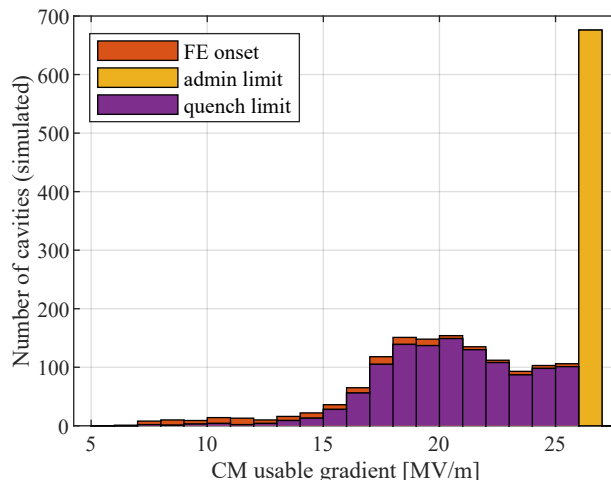

Figure 4: Usable gradient limit distribution for simulation with parameters emulating observed LCLS-II-HE vertical test performance and improved gradient degradation factors.

MODELING LCLS-II-HE

Turning to the new project now underway, LCLS-II-HE has some notable differences from its predecessor LCLS-II. Relevant to this work, the target cryomodule gradient is 21 MV/m compared to the earlier 16 MV. The administrative limit in cryomodule tests has been increased to 26 MV/m. Some changes have been made to the cavity preparation protocol, including the improvement of temperature control during electropolishing, that have been shown to improve the peak gradient performance of the cavities [7]. Moreover, an explicit effort to identify and process multipacting in vertical test and cryomodule test is being implemented. Indeed, the vertical test results of the ten cavities prepared by an industrial vendor for the LCLS-II-HE verification cryomodule (vCM) averaged a peak gradient of 25.6 ± 1.1 MV/m [8]. Further improvements have been made to the handling and assembly procedures and infrastructure to reduce the introduction of field emitters (*e.g.* dust on the cavity surface). The eight cavities installed in the vCM, selected from the above ten cavities and assembled using these improved procedures, have recently been shown to reach an average usable gradient of 24.4 ± 1.1 MV/m with a minimum of 23.1 MV/m [8]. Multipacting was observed on most of the cavities in the 17-22 MV/m range, but was conditioned away by quench processing. One vCM cavity exhibited a small amount of field emission which later processed away; the rest showed no field emission [1].

Based on the improvements implemented for LCLS-II-HE and the success of the vCM, we can repeat the above simulation with modified parameters to get an idea of how LCLS-II-HE cryomodules might perform. We can decrease the total defect density parameter *s* to 5.5, resulting in an average vertical test gradient of 25.6 MV/m and consistent with the supposition that the improvements to the cavity surface treatment result in a lower number of defects [7]. We can also reduce the simulated rates of field emission and

multipacting to account for the improvements in assembly and handling procedures and the heightened focus on identifying and processing multipacting. Finally, we can raise the administrative limit to the new value of 26 MV/m.

Figure 4 shows the results of one such simulation, with a quite positive outcome. Here the rates of gradient limitation by multipacting and field emission have each been reduced by half compared to the LCLS-II results above (these are modest improvements, given that none of the vCM cavities were limited in usable gradient by multipacting or field emission). The vertical test acceptance threshold has intentionally been omitted to better understand the usable gradient distribution. In this scenario, 60% of all cavities, including those that might have been rejected after vertical test due to low peak gradients, have usable gradients above the target of 21 MV/m. More than 30% of cavities are limited only by the administrative limit. The mean usable gradient of all cavities is 21.8 MV/m, exceeding the target for LCLS-II-HE.

Imposing a vertical test gradient acceptance threshold improves all these metrics. Figure 5 shows the simulated vertical test peak gradient of the same set of cavities in blue, sorted in descending order. The red line shows the cumulative mean usable gradient achieved in the assembled cryomodules by rejecting cavities with peak vertical test gradients worse than the given cavity. For example, to read from the figure, setting an acceptance threshold of $E_{acc} = 22$ MV/m would result in the rejection of approximately 20% of cavities after vertical test, with a mean usable gradient in the cryomodules of 23 MV/m. The cumulative mean never drops below 21 MV/m, so at least from the standpoint of usable gradient, all cavities could be used with no vertical test acceptance threshold while still achieving the target mean usable gradient.

It is also prudent to project how the LCLS-II-HE cavities might perform if the improvements to field emission and

---

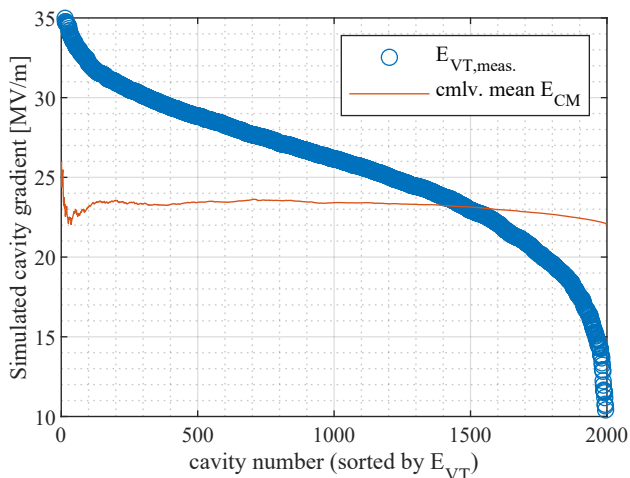[1] The full results of the vCM test will be published in future material.

Figure 5: Blue points show the simulated results of the accelerating gradient observed in vertical test; cavities are sorted by this gradient in descending order. Red line shows the cumulative mean usable gradient in the cryomodule if accepting all cavities in this order. Simulation results correspond to those shown in Fig. 4.
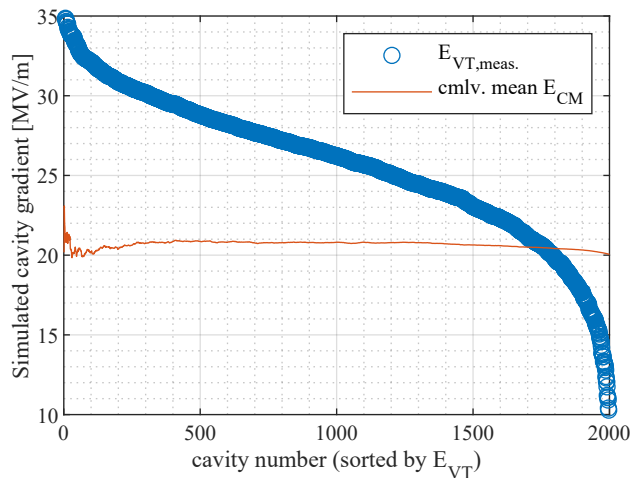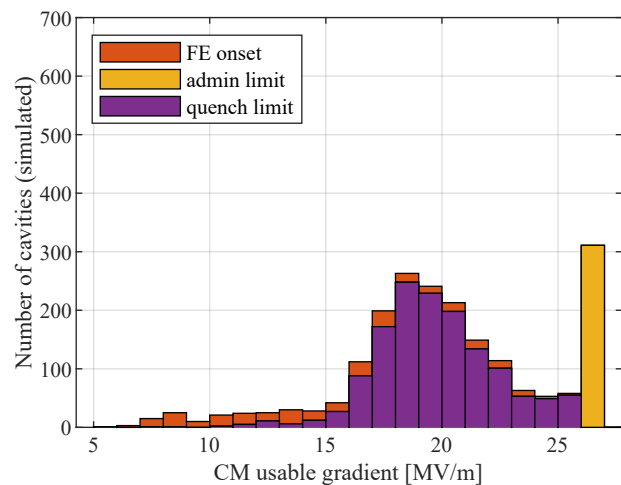

Figure 6: Usable gradient limit distribution for simulation with parameters emulating observed LCLS-II-HE vertical test performance and gradient degradation factors consistent with LCLS-II.

multipacting processing are not as dramatic. Figure 6 shows the results of a simulation with the same improved vertical test performance shown in Fig. 4 but with the same rates of limitation by multipacting and field emission observed in LCLS-II. Here, only 37% of the cavities have usable gradients above 21 MV/m, and overall the cavities have a mean usable gradient of 20.0 MV/m. Only about 15% of the cavities reach the administrative limit. As above, these metrics could be improved by the imposition of a vertical test gradient acceptance threshold.

Figure 7 shows the sorted cavity plot of these results. It is clear that the mean usable gradient is lower across the board, no matter where the gradient acceptance threshold might

Figure 7: Same presentation as in Fig. 5. Simulation results correspond to those shown in Fig. 6.

be set. Indeed there is no feasible acceptance threshold that would allow a mean usable gradient meeting the 21 MV/m target.

VARIABLE ACCEPTANCE THRESHOLD FOR ACCELERATING GRADIENT

As illustrated above, the final mean usable gradient of the LCLS-II-HE cryomodules may be strongly impacted if multipacting and field emission are prevalent. The very promising results from the vCM suggest that this will not be the case, but it will be important to track these phenomena over the course of production to ensure the accelerator meets its performance target and simultaneously avoid unnecessary rework and rejection of cavities.

The project has chosen an initial vertical test gradient acceptance threshold of 23 MV/m based on the vCM results and allowing for a 5% uncertainty range in the measurement of the accelerating gradient. The LCLS-II-HE cavity technical board (CTB), a collection of subject matter experts representing SLAC, JLab, and FNAL, is tasked with overseeing the technical aspects of cavity production and approving cavities for inclusion in cryomodule strings. Over the course of the project the CTB will carefully track vertical test and cryomodule test data as it becomes available. Using this data the CTB will monitor the degradation of gradient through the mechanisms outlined in this study. As outlined in internal LCLS-II-HE project documentation [9], the CTB will periodically perform the simulation described above using parameters consistent with the incoming test results in order to anticipate the performance of cavities to come.

If deemed necessary, the CTB has the ability to impose a variable acceptance threshold for the accelerating gradient. This could result in raising the threshold, if for example gradient degradation between vertical test and cryomodule test is stronger than anticipated and early cryomodules do not achieve adequate levels of performance; it could also result in lowering the acceptance threshold if cryomodules

perform very well and there are enough high-performing cavities to allow cavities which do not individually meet the 21 MV/m specification. In the most dynamic case, the CTB may choose to adjust the gradient acceptance threshold after every or every other cryomodule; this would likely only be the case if there is a wide spread in cavity gradient performance and costs associated with rejection or rework of cavities become a concern.

ADDENDUM

An earlier treatment of this model which goes into some additional detail was presented in a 2020 SLAC engineering note [10].

REFERENCES

[1] D. Gonnella *et al.*, "Industrialization of the nitrogen-doping preparation for SRF cavities for LCLS-II," *Nucl. Instrum. Methods Phys. Res., Sect. A*, vol. 883, pp. 143–150, Mar. 2018. `doi:10.1016/j.nima.2017.11.047`

[2] H. Safa, "Statistical analysis of the quench fields in SCRF cavities," in *Proc. SRF'97*, Padova, Italy, Oct. 1997, paper SRF97C11, pp. 503–509.

[3] J. T. Maniscalco, "Studies of the field-dependent surface resistance of nitrogen-doped niobium for superconducting ac-celerators," Ph.D. thesis, Cornell University, Ithica, NY, USA, 2020.

[4] T. Powers, "Theory and practice of cavity RF test systems," in *Proc. SRF'05*, Ithaca, NY, USA, Jul. 2005, paper SUP02, pp. 40–70.

[5] O. Melnychuk, A. Grassellino, and A. Romanenko, "Error analysis for intrinsic quality factor measurement in superconducting radio frequency resonators," *Rev. Sci. Instrum.*, vol. 85, pp. 124705, Dec. 2014. `doi:10.1063/1.4903868`

[6] P. Yla-Oijala, "Electron multipacting in TESLA cavities and input couplers," *Part. Accel.*, vol. 63, pp. 105–137, 1999.

[7] D. Gonnella, "SRF R&D for the LCLS-II high energy upgrade," presented at LINAC'20, Liverpool, UK. Sept. 2020, unpublished.

[8] D. Gonnella, "The LCLS-II-HE High Q0 and Gradient R&D Program," presented at SRF'21, Grand Rapids, MI, USA, Jun.-Jul. 2021, paper TUPFDV003, this conference.

[9] J. T. Maniscalco, "LCLS-II-HE VT acceptance test procedure and criteria," SLAC, Menlo Park, CA, USA, Rep. LCLSII-HE-1.2-PP-0356-R0, 2021.

[10] J. T. Maniscalco, "A path for establishing the vertical test accelerating gradient acceptance threshold," SLAC, Menlo Park, CA, USA, Rep. LCLSII-HE-1.2-EN-0247-R0, 2020.